Photon Netw Commun (2015) 29:67–77
DOI 10.1007/s11107-014-0467-x

Mapping time-varying IP traffic to flexible optical paths in flexgrid optical networks

Caglar Tunc · Nail Akar

Received: 13 March 2014 / Accepted: 25 July 2014 / Published online: 28 August 2014

Abstract A spectrum slot is the frequency range allocated to a single channel within a flexible grid, and its width needs to be an integer multiple of the so-called slot width granularity. The slot width of the spectrum slots to be used for an optical path in flexgrid optical networks can be adjusted in time to align with time-varying client traffic demand for both bandwidth and energy efficiency purposes. However, frequent adjustment of the slot width of optical paths places substantial signaling load on the control plane. In this paper, an online slot width adjustment mechanism is proposed for flexgrid optical networks under slot width update rate constraints in order to maintain the associated signaling load at acceptable levels. Real traffic traces are used to validate the effectiveness of the proposed mechanism.

Keywords Flexgrid optical networks · Dynamic slot width adjustment · Elastic spectrum allocation · IP over optical architectures

1 Introduction

Optical transport networks currently use Dense Wavelength Division Multiplexing-based (DWDM) transmission using the International Telecommunication Union (ITU) fixed frequency grid, which divides the optical spectrum range at the C-band (1,530–1,565 nm) into fixed 50-GHz spectrum slots [15,26]. In fixed-grid optical networks, the basic switching unit is a wavelength, which has fixed bandwidth. For transmissions beyond 100 Gbps, ITU (International Telecommunications Union) has defined the flexible frequency grid (flexgrid in short) [16]. The concept of a variable-size frequency slot (or spectrum slot) is introduced in flexgrid to describe the frequency range allocated to a single channel, which is characterized by its nominal central frequency (CF) and its required slot width (SW) values. For the flexgrid, an allowed spectrum slot characterized by the pair (n, m) has a nominal central frequency defined by CF = 193.1 THz + $n\Delta_f$ for an integer n and SW = $\Delta_c m$ in units of GHz for a positive integer m where Δ_f is the nominal CF granularity and Δ_c is the SW granularity. In [16], $\Delta_f = 6.25$ GHz and $\Delta_c = 2\Delta_f = 12.5$ GHz. The slot width (or the channel size) is then expressed in terms of m basic channel segments where a segment width is Δ_c [19]. Throughout this paper, we will use the notation SW = m in units of segments given that Δ_c is fixed.

Core network providers have been looking into alternatives of transporting IP (Internet Protocol) traffic over optical networks. The present mode of operation relies on IP over DWDM where packet processing is performed electronically at a router and one or several wavelengths are dedicated to a pair of routers [27]. More futuristic architectures rely on optical packet or burst switching that allow bandwidth sharing at a granularity finer than a full wavelength [3,29]. Flexgrid optical networks (FG-ON), the focus of the current paper, provide a new alternative to IP transport over optics where a connection between two routers can flexibly change its bandwidth over the lifetime of the connection and the associated spectrum [14]. Two key enabling technologies are crucial for the realization of FG-ONs: Bandwidth-Variable Transponders (BV-T) and Bandwidth-Variable Optical Cross-Connects (BV-OXC). A BV-T maps the client traffic to an optical signal with an appropriate modulation order using a frequency

C. Tunc · N. Akar (✉)
Electrical and Electronics Engineering Department, Bilkent University, Ankara, Turkey
e-mail: akar@ee.bilkent.edu.tr

C. Tunc
e-mail: caglar@ee.bilkent.edu.tr

slot with just enough resources to serve the client's needs. On the other hand, in contrast with fixed-grid optical networks, a BV-OXC switches variable-sized frequency slots from an input port to another port. Use of BV-Ts and BV-OXCs has been demonstrated in the SLICE network using orthogonal frequency division multiplexing (OFDM) [18]. For more detailed study of BV-Ts and BV-OXCs and their experimental demonstration, the reader is referred to [12,13], and [18]. Also, we refer the reader to a recent survey on OFDM-based elastic optical networks [38]. The focus of our work in this paper is the client traffic mapping functionality of BV-Ts.

Although current 100 Gbps transmission systems are able to use the current fixed grid, higher bit rate super-wavelength signals (including 400 Gbps and 1 Tbps signals) can not fit into a fixed slot at standard modulation formats [15,17,18]. On the other hand, low bit rate signals, i.e., sub-wavelength, can not be transported efficiently in the optical domain using fixed size slots. FG-ONs allow both low and high bit rate signals in the same infrastructure using variable-size frequency slots. A flexible or elastic optical path (flexi-path in short) refers to an optical path consisting of the nodes and links between the two ends of the network occupying a variable-size frequency slot within the entire spectrum. Moreover, in FG-ONs, the channel size for the optical connection and the type of modulation can be determined on the basis of distance between the transmitter and receiver [17], time-varying physical impairments [13], or on time-varying traffic demands [19]. Each of the adaptation methods described above presents advantages in terms of overall bandwidth and energy use. The focus of our work in this paper is the traffic-adaptive feature of FG-ONs.

The capability to allocate spectrum resources elastically according to traffic demands is crucial for FG-ONs [19]. Three types of spectrum allocation (SA) methods for a flexi-path are defined in [19]. In fixed SA (FSA), both the assigned CF and SW to the flexi-path do not change with time. Therefore, the SW needs to be chosen at the flexi-path establishment phase so as to meet the largest potential traffic demand in its lifetime. In Semi-Static SA (SSSA), the assigned CF to the flexi-path is fixed, but its SW is allowed to change in time so as to align with the traffic demand. Since spectrum can only be shared between neighboring demands, statistical multiplexing gains would be very limited with SSSA. However, energy can be saved in SSSA in case of lower traffic demands. The most flexible scenario is ESA (elastic spectrum allocation) where both the assigned CF and SW are allowed to change in time. We consider ESA in this paper due to its bandwidth efficiency, but its implementation issues are left for future research. However, conceptually, when the flexi-path requires a frequency slot width update in the context of ESA, it will send an update request to the network which in turn will check the idle spectrum resources to make a decision on the new CF and SW. The allocated spectral resources need to be the same along the links in the route (the continuity constraint) if spectrum conversion is not possible at the BV-OXCs, and contiguous in the spectrum (the contiguity constraint) [30]. The problem of finding a route and spectral resources to satisfy the needs of the ESA request is known as routing and spectrum allocation (RSA) problem [30]. The more general problem of routing, modulation level and spectrum allocation (RMLSA) problem is studied in [9] using ILP formulation and simulated annealing meta-heuristic. For more details on RSA and the related spectrum fragmentation problem, we refer the reader to [8,9,28,33–35]. For signaling purposes, Internet Engineering Task Force (IETF) is currently working on the distributed control plane for FG-ONs and in particular the flexgrid extensions to existing signaling protocols for Internet Protocol (IP) traffic [11,37]. Centralized openflow-based control plane for FG-ONs is also being considered [39]. In any case, too often flexi-path SW update requests would place a burden on the control plane. Therefore, update request rates also need to be taken into account. Our goal in this paper is to develop an online mechanism for mapping time-varying IP traffic to a flexi-path whose SW changes in time while adapting to traffic but without having to exceed a certain desired SW update rate. We also present a variation of this online mechanism, which maintains a tolerable loss rate based on online loss measurements. These proposed mechanisms are validated by actual traffic traces. Dynamic bandwidth allocation in electronically switched networks has been studied extensively while taking into account of the signaling costs associated with allocation updates [21,23–25] for ATM (Asynchronous Transfer Mode) networks, [2] for bandwidth brokers in IP networks, [20,22] for general wide area networks, [1,10] for MPLS (Multi Protocol Label Switching) networks. To the best of our knowledge, the problem of dynamic bandwidth allocation under signaling constraints in the context of FG-ONs has not been studied in the literature, which is the scope of the current paper.

We focus on a single flexi-path in this paper, and we do not consider SW update request blocking in the FG-ON due to lack of spectral resources. Our goal is to characterize the gain in bandwidth stemming from the use of a single flexi-path assuming a well-provisioned FG-ON that admits all requests. We leave it for future research to quantify the gain (in terms of overall network cost, for example) that can be obtained by traffic adaptation in FG-ONs of realistic topologies supporting many flexi-paths. Note that in the network scenario, it will be possible that a SW update request would be blocked due to lack of continuous and contiguous spectrum, which makes the network scenario more challenging than the single flexi-path scenario considered in this paper. To reduce blocking and harvest network gains, there is an increased need for deployment of effective spectrum allocation mechanisms

with fragmentation avoidance such as the ones proposed in [32,36] and also routing methods such as [9,31] in heterogeneous FG-ONs.

The paper is organized as follows. Section 2 describes the proposed scheme for mapping time-varying IP traffic to a flexi-path. We present our numerical results in Sect. 3. We conclude in the final section.

2 Online slot width adjustment

In this section, we will introduce the online slot width adjustment (OSWA) mechanism we propose for mapping time-varying IP traffic to flexi-paths in terms of updating the SW of the frequency slot in units of segments upon traffic changes in the context of ESA. Finding the CF of the spectrum slot on each path so that the frequency slot is allocated on each link of the flexi-path is left outside the scope of this paper.

Toward the description of OSWA, we let β denote the desired maximum number of SW updates per unit time. The reciprocal of β is denoted by T_u, which is the desired minimum average time between two SW updates. It is the goal of OSWA that the average inter-update times should be lower bounded by T_u. Moreover, decisions to make SW updates or not are made at integer multiples of a basic measurement period denoted by T_m. Let R_k (in units of bps) denote the average data rate demand of the client IP layer in the time interval $((k-1)T_m, kT_m), k \geq 1$. This IP layer traffic is to be mapped to a flexi-path for which the SW required by the flexi-path at the same time interval $((k-1)T_m, kT_m)$ denoted by Z_k in units of segments is given by:

$$Z_k = \frac{R_k}{B_{\text{mod}}\Delta_c}, \tag{1}$$

where Δ_c denotes the slot width granularity in GHz and B_{mod} (in bits/s/Hz) is the spectral efficiency of the chosen modulation format [5]. For instance, the spectral efficiency of the 16-QAM modulation format is denoted by $B_{\text{16-QAM}}$, which is 4 bits/s/Hz, whereas QPSK has a spectral efficiency of $B_{\text{QPSK}} = 2$ bits/s/Hz [5]. Note that Z_k is real-valued and since SW must be integer-valued in units of segments, $\lceil Z_k \rceil$ is actually the minimum number of segments necessary to meet the traffic demand R_k. In the above definition, $\lceil Z_k \rceil$ is the smallest integer larger than or equal to Z_k. Based on the update decision made at instant $t = kT_m$, S_{k+1} segments are used to form the spectrum slot in the time interval $(kT_m, (k+1)T_m), k \geq 1$ during which the channel capacity (in units of bps) will be equal to $S_{k+1}B_{\text{mod}}\Delta_c$. If $S_{k+1} \neq S_k$; then, a SW update is said to take place at time $t = kT_m$. In this setting, loss of information is inevitable since the flexi-path capacity may occasionally fall short of the demand. Neglecting the impact of buffering, we use the following identity in this paper to characterize the loss denoted by L:

$$L = \frac{\int_{t=0}^{T} \max\left(0, R(t) - S(t)B_{\text{mod}}\Delta_c\right) \mathrm{d}t}{\int_{t=0}^{T} R(t)\mathrm{d}t}, \tag{2}$$

where T is the time over which the measurements would be performed, the continuous-time functions $R(t)$ and $S(t)$ denote the instantaneous data rate and the number of segments used, respectively, at time t. Similarly, we define the real-valued continuous-time function $Z(t)$ as the segment requirement at time t, i.e.,

$$Z(t) = R(t)/(B_{\text{mod}}\Delta_c).$$

However, note that a sampled version of $R(t)$ denoted by $R^{(j)}$ is generally available, which denotes the demanded bit rate in the interval $((j-1)T_s, jT_s)$ for $j \geq 1$ for a choice of sampling period $T_s \leq T_m$. Also let $S^{(j)}$ denote the number of segments used in the same time interval $((j-1)T_s, jT_s)$. Consequently, the expression for the loss rate L reduces to

$$L = \frac{\sum_{j=1}^{N} \max\left(0, \left(R^{(j)} - S^{(j)}B_{\text{mod}}\Delta_c\right)\right)}{\sum_{j=1}^{N} R^{(j)}}, \tag{3}$$

where N is the total number of sampling periods over which measurements are performed. In our numerical examples, we set the sampling period T_s to 1 s. unless stated otherwise and we use the expression (3) for loss rate calculations. Given $R_{\max} = \max_j R^{(j)}$, which is generally known a-priori, $S_{\max}$ represents the largest possible slot width to be used for this data stream. In particular,

$$S_{\max} = \left\lceil \frac{R_{\max}}{B_{\text{mod}}\Delta_c} \right\rceil. \tag{4}$$

We also define a gain metric G to describe the percentage gain in using OSWA as opposed to using a fixed number of $S_{\max}$ segments irrespective of the time-varying nature of the client IP traffic. Mathematically,

$$G = \frac{\sum_{k=1}^{M}(S_{\max} - S_k)}{S_{\max}M}100, \tag{5}$$

where M is the total number of measurement periods over which the gain measurements are to be performed. The gain G is indicative of savings in terms of both bandwidth and energy.

A crucial component of OSWA is a leaky bucket that we propose to keep track of SW updates. The bucket occupancy is denoted by B_k at time $t = kT_m$. At each measurement period $t = kT_m$, the bucket occupancy is decremented by an amount that equals $\kappa\beta T_m$ until the bucket occupancy hits zero, i.e., $B_k = \max(0, B_{k-1} - \kappa\beta T_m)$, where κ is a free bucket parameter. We define a band with lower threshold

$D_k = S_k - B_k$ and upper threshold S_k at time $t = kT_m$. We also define $D(t)$ that is obtained through a linear interpolation of the sample values D_k, i.e., $D(kT_m) = D_k, k \geq 0$. At time $t = kT_m$, a decision is made for a SW update if the following condition is met:

$$Z_k \notin [D_k, S_k] \text{ or } Z_k > S_k \tag{6}$$

Each time epoch this condition is met is called a potential SW update epoch. At each actual SW update, the bucket is incremented by κ but not beyond a certain bucket size denoted by $B_{\max}$. Algorithm 1 completely describes the OSWA slot width adjustment mechanism we propose for a given traffic stream characterized with the random sequence $R_k, k \geq 1$. The illustration of OSWA in an example scenario for $T_m = 144$ s and $T_u = 120$ min is given in Fig. 1. In this example, the daily trace (sampled with a sampling period of $T_s = 144$ s) is obtained from a 10 GigE link from Chicago to Seattle from CAIDA (The Cooperative Association for Internet Data Analysis) on August 29–30, 2011 [4]. The maximum bit rate observed in the original trace is equal to 3.491 Gbps, and we scaled up the original trace by a factor of 28.643 so that the maximum bit rate of the modified trace became 100 Gbps. We use $S_{\max} = 8$ and the bucket parameter κ is set to unity in this example. As seen in this example, the total number of SW updates on this daily trace is twelve, which is in compliance with the desired T_u. Moreover, the SW selection mechanism provides an upper envelope for the demand where the allocation rarely falls short of meeting the demand.

Algorithm 1: OSWA Online slot width adjustment algorithm.

Input: Instantaneous data rate R_k
Output: Segment allocation S_{k+1}
initialization $k = 0$, $B_0 = \frac{B_{\max}}{2}$, $S_0 = S_{\max}$
while *True* **do**
  $k \leftarrow k + 1$
  $Z_k \leftarrow \frac{R_k}{B_{\text{mod}}\Delta_c}$
  $B_k \leftarrow max(0, B_{k-1} - \kappa\beta T_m)$
  $D_k \leftarrow S_k - B_k$
  if $Z_k \notin [D_k, S_k]$ or $Z_k > S_k$ **then**
    $S_{k+1} \leftarrow min(S_{\max}, \lceil Z_k \rceil)$
    if $S_{k+1} \neq S_k$ **then**
      $B_k \leftarrow min(B_{\max}, B_k + \kappa)$
  else $S_{k+1} \leftarrow S_k$
  return S_{k+1}

OSWA tries to keep the bucket occupancy away from the two terminal points zero and $B_{\max}$, which ensures that the actual SW update rate would be close to the desired update rate β. One caveat for OSWA is that the actual loss delivered by OSWA may be high depending on the choice of the measurement period T_m. Large values of T_m lead to a large gain G but also to a relatively large loss rate L. On the other hand, small values for T_m yield a low loss rate L but present marginal bandwidth gain G. Therefore, the choice of T_m is critical for the success of OSWA to attain a certain tolerable loss rate L_T. We therefore propose the loss-controlled version of OSWA, namely LC-OSWA (Loss-Controlled OSWA), which dynamically adjusts the measurement period T_m based on loss measurements with the intention of keeping the actual loss rate L around a predetermined tolerable loss rate L_T. For this purpose, we introduce an observation period T_o during which we propose to use OSWA with fixed T_m. At the end of each observation period T_o, we calculate the loss rate during the observation period, which is denoted by $\hat{L}$. Based on the measurement, the measurement period T_m is updated for the next observation period. The process repeats itself where values of T_m in two different observation periods may be different. In LC-OSWA, we allow the measurement period T_m to be lower (upper) bounded by $T_{\min}$ and ($T_{\max}$). We also have dynamically maintained lower (upper) bounds T_- (T_+) for T_m. The main idea of LC-OSWA is to adjust T_m by binary search in the shrinking band of values between T_- and T_+ according to the most recent $\hat{L}$. However, due the fact that outcomes in each observation period are random due to the randomness of traffic patterns, the band of values over which a search is performed is allowed to expand once the band vanishes. Let h denote the time interval $((h-1)T_o, hT_o)$, i.e., hth observation period for $h \geq 1$. Algorithm 2 completely describes the LC-OSWA slot width adjustment mechanism we propose. In the algorithm description, we use the

Algorithm 2: LC-OSWA loss-controlled online slot width adjustment mechanism.

Input: Tolerable loss rate L_T, observation period T_o
Output: Measurement period T_m
initialization $h = 1$
while *True* **do**
  Use OSWA for slot width adjustment with measurement period fixed to T_m for the current observation period
  Calculate the loss rate $\hat{L}$ for the current observation period
  if $\hat{L} > L_T$ **then**
    $T_+ \leftarrow T_m$
    $T_m \leftarrow max\left(T_{\min}, T_s \left\lfloor \frac{T_m + T_-}{2T_s} \right\rfloor\right)$
  else if $\hat{L} < L_T$ **then**
    $T_- \leftarrow T_m$
    $T_m \leftarrow min\left(T_{\max}, T_s \left\lfloor \frac{T_m + T_+}{2T_s} \right\rfloor\right)$
  if $T_- = T_+$ **then**
    $T_- \leftarrow max\,(T_{\min}, T_- - \Delta)$
    $T_+ \leftarrow min\,(T_{\max}, T_+ + \Delta)$
  return T_m
  $h \leftarrow h + 1$

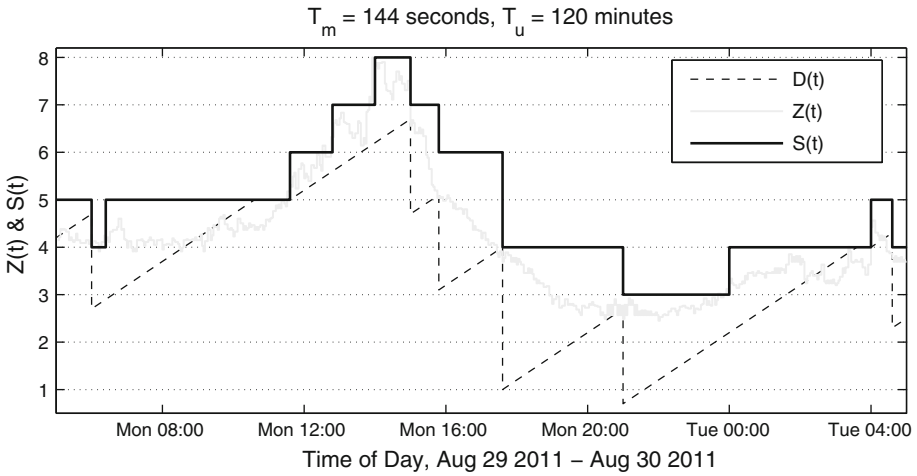

Fig. 1 Illustration of the operation of OSWA in an example scenario for measurement period $T_m = 144$ s and $T_u = 120$ min

notation $\lfloor X \rfloor$ to represent the largest number less than or equal to the real number X. For convenience, we force all algorithm parameters to be integer multiples of the basic time unit T_s, namely the parameters $T_{\min}$, $T_{\max}$, T_-, T_+, and Δ.

3 Numerical examples

Three real-world traffic traces, two from the MAWI repository [6,7], and one from the CAIDA archives [4] are used to assess the two proposed slot width adjustment algorithms, namely OSWA and LC-OSWA. *Trace 1*, which is 50-h-15-min-long, is taken from a 150-Mbps trans-Pacific line on January 9, 2007, whereas *Trace 2*, a 24-h-long trace, is taken from a 10-Mbps trans-Pacific line on March 3, 2006. Both traces originally have a sampling period $T_s = 1$ s. Traces 1 and 2 are then scaled up to 100 Gbps by multiplying the $R^{(j)}$ values of the original traces by a factor of 666.67 and 10,000, respectively, to obtain two 100 Gbps data streams. On the other hand, *Trace 3* is obtained from the 100 Gbps trace we used in Fig. 1, which has a sampling period of $T_s = 144$ s. For the purpose of obtaining an upsampled data stream with $T_s = 1$ s, we add zero mean Gaussian noise to this 100 Gbps trace with a standard deviation of 3 Gbps to obtain the one-day long Trace 3. With the way the three traces are obtained, traces 1, 2, and 3 possess an average data rate of 45.66, 75.67, and 52.13 Gbps, respectively, all having a maximum bit rate $R_{\max} = 100$ Gbps. For simulation studies, all three traces are wrapped around themselves ten times to obtain longer traces. Then, the SW adjustment schemes are simulated using $T_s = 1$ s for loss rate calculations. In our numerical examples, we assume a segment width of $\Delta_c = 6.25$ GHz and two different modulation formats, namely QPSK and 16-QAM, yielding two different values for $S_{\max} = 8$ ($S_{\max} = 4$) when QPSK (16-QAM) is used. Moreover, in Example 3, we also study the case $S_{\max} = 12$ to observe the impact of $S_{\max}$ on system performance. We take the bucket parameter $\kappa = 1$ in all the numerical examples. The unit for the parameter β is taken to be updates/hour throughout all the numerical examples. For convenience, some of the algorithm parameters are provided in Table 1.

Table 1 Summary of some of the parameters used in algorithms OSWA ad LC-OSWA

Parameter	Definition	Value
β	SW update rate	Variable (updates/h)
T_u	Reciprocal of β	Variable
T_s	Sampling period of the original traces	Set to 1 s
T_m	Measurement period	Fixed in OSWA, variable in LC-OSWA
T_o	Observation period	Set to 1 h
$S_{\max}$	Maximum SW value	4, 8, or 12
L	Loss rate calculated using (3)	Variable
L_T	Tolerable loss rate for LC-OSWA	Variable in the range 0.0005 - 0.01

3.1 Example 1

In the first example, we set $T_m = 100$ s and the time-varying traffic demand represented by the quantity $Z(t)$ and the slot width $S(t)$ produced by OSWA is depicted in Figs. 2 and 3 for $\beta = 2, 8$ for trace 1, and for $\beta = 1, 3$ for trace 2. This process is repeated for trace 3 in Fig. 4 while this time T_m being set to 12 s. In all plots, Z_k values are used and not $Z^{(j)}$. These plots are presented to help the reader in visualizing the three traces including the upsampling process used for trace 3 and in understanding how the OSWA algorithm works in practice for real traffic traces.

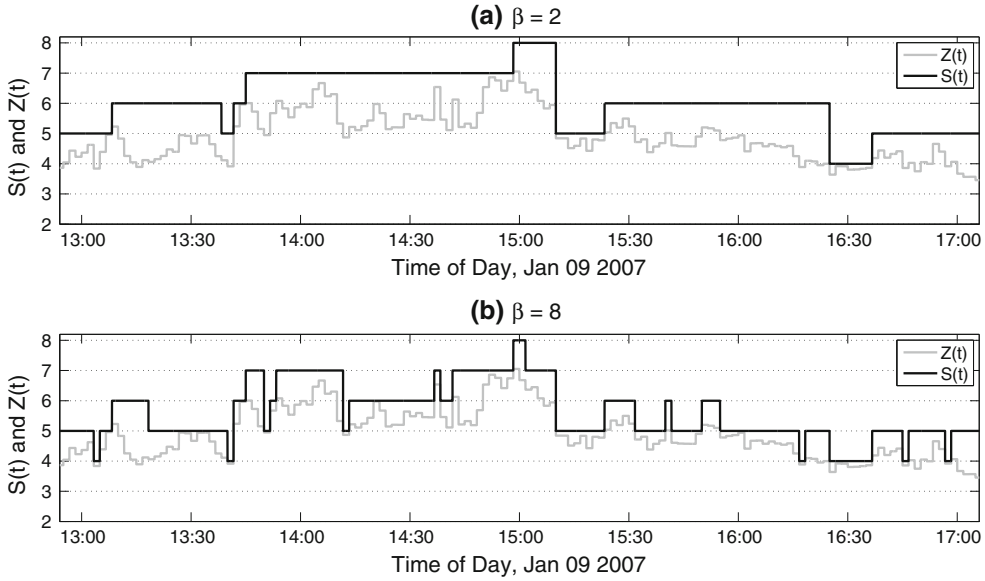

Fig. 2 The traffic demand $Z(t)$ and the slot width $S(t)$ as dictated by OSWA for trace 1 **a** $\beta = 2$, **b** $\beta = 8$ for a 4-h time window with T_m=100 s

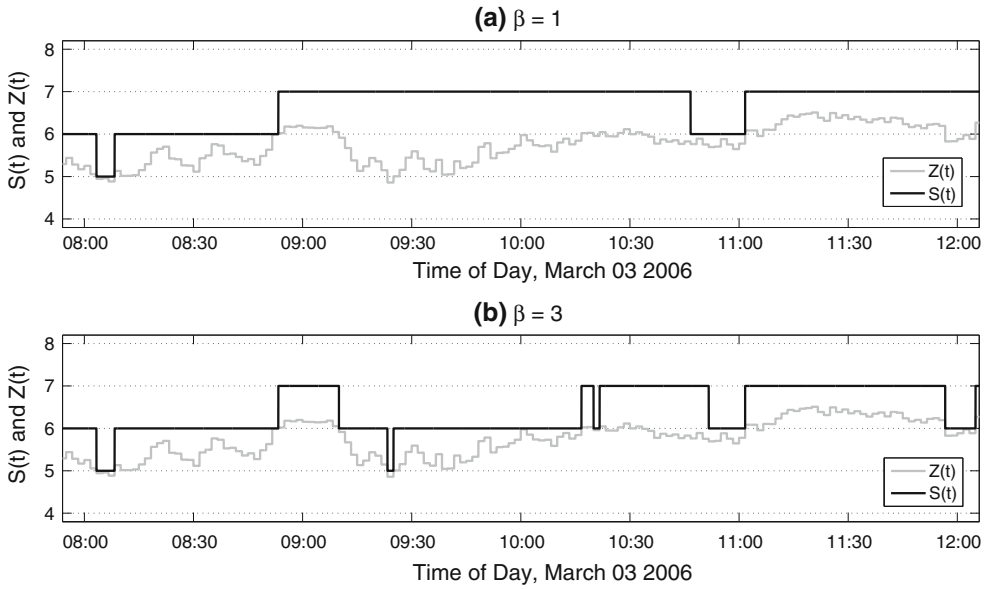

Fig. 3 The traffic demand $Z(t)$ and the slot width $S(t)$ as dictated by OSWA for trace 2 **a** $\beta = 1$, **b** $\beta = 3$ for a 4-h time window with T_m=100 s

3.2 Example 2

In this section, we study the OSWA scheme by the simulation of OSWA for three traces for T_m values varying between T_s and T_u when $S_{\max}$ is set to 8. Out of all simulation runs, we then obtain the particular value of T_m, denoted by T_m^*, for which the simulated loss rate L is attained at a certain level. For various loss rate levels, we obtain the particular percentage gain G, denoted by G^*, which is obtained when OSWA is to employ the particular value of $T_m = T_m^*$. Note that the parameters T_m^* and G^* depend on the actual loss rate L. Our numerical results are presented in Fig. 5 in which the gain G^* and measurement period T_m^* values are depicted as a function of the desired update rate β for all three traces and for different values of L. We have the following observations.

- Even when T_m takes its maximum value at T_u, the loss rate does not exceed 0.005 for all values of β we study for traces 2 and 3. Therefore, we do not depict the results for $L \geq 0.005$ for these traces since lower loss rates are attained with the immediate choice of $T_m = T_u$.
- For a given attainable loss rate, the gain in using OSWA increases by the update rate β. In light of the results for

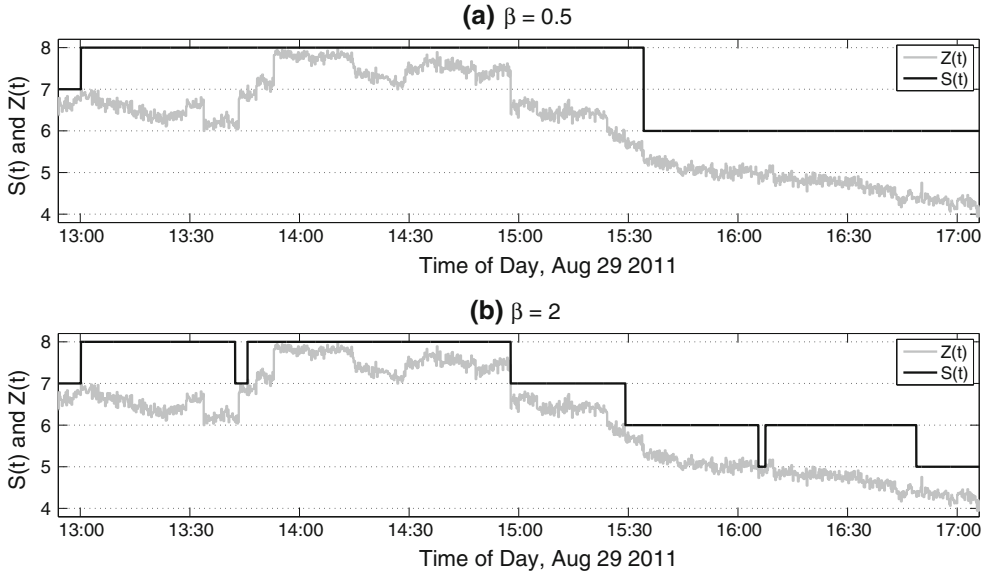

Fig. 4 The traffic demand $Z(t)$ and the slot width $S(t)$ as dictated by OSWA for trace 3 **a** $\beta = 0.5$, **b** $\beta = 2$ for a 4-h time window with T_m=12 s

both traffic traces, the majority of this gain is attained for β in the proximity of five to ten updates/hour with marginal gains when β is increased further.

- Traces 1 and 3 present higher gains than trace 2, which has a higher average rate than the other two, and it is clear that lightly loaded links would benefit more with OSWA. To further explain this observation, consider an hypothetical offline mechanism that allocates segments to the data streams at every $T_s = 1$ s. ensuring zero loss rate. For the case $S_{\max} = 8$, the hypothetical offline mechanism would require 4.15, 6.59, and 4.66 segments on the average for traces 1, 2, and 3, respectively. This means that with zero loss rate, the maximum amount of gain G attainable with the hypothetical scheme is 48.11, 17.63, and 41.72 %, respectively, for traces 1, 2, and 3. Note that these values provide an upper bound to what OSWA can deliver and the upper bound for trace 2 is much lower than those of traces 1 and 3, which explains the relatively low OSWA performance with trace 2. Also note that OSWA delivers performance very close to these upper bounds for relatively high loss rates and an update rate satisfying $\beta \geq 5$.
- Relaxing the loss constraint has a significantly positive impact on the attainable gain for a given β. Therefore, if advantages of flexible optical networking are to be enjoyed, then increased losses need to be tolerated.
- The measurement period T_m^* for a given attained loss rate L depends on L and the choice of β. In particular, T_m^* decreases with increasing β and also decreases with decreasing L. Actually, it is this observation that has led us to propose LC-OSWA, which varies the measurement period T_m on the basis of actual loss rate measurements.

3.3 Example 3

In the third example, we plot G^* as a function of the loss rate L, which is allowed to vary from 0.0005 to 0.01 and 0.0005 to 0.004 for traces 1 and 3, respectively; but this time for three different values of $S_{\max} = 4, 8, 12$ and for $\beta = 6$ for both traces in Fig. 6. It is clear that increased $S_{\max}$ enhances the gain for a given loss rate L, but the majority of the gain is achievable with $S_{\max} = 8$ with marginal improvement when $S_{\max}$ is further increased. Moreover, the OSWA gain is reduced steadily when the attained loss rate is reduced.

3.4 Example 4

Although OSWA leads to significant gains, this is only possible with a proper choice of the measurement period T_m. LC-OSWA described in Algorithm 2 is proposed for this purpose, which automatically adjusts T_m based on loss measurements so as to attain a certain tolerable loss rate L_T. In this final example, LC-OSWA is studied for traffic traces 1 and 3, for various values of L_T. The observation period T_o is set to 1 h. When the LC-OSWA parameter Δ is relatively large, changes in the traffic pattern are detected rapidly at the expense of relatively poor steady state behavior for T_m. In LC-OSWA simulations, we set $\Delta = 1$ s. We also set $T_{\max} = T_u/2$ and $T_{\min} = 1$ s. For varying values of β, we compare the gain and the actual SW update rate obtained by the online algorithm LC-OSWA with those obtained based on OSWA in Tables 2, 3, 4 and 5. Note that in this example,

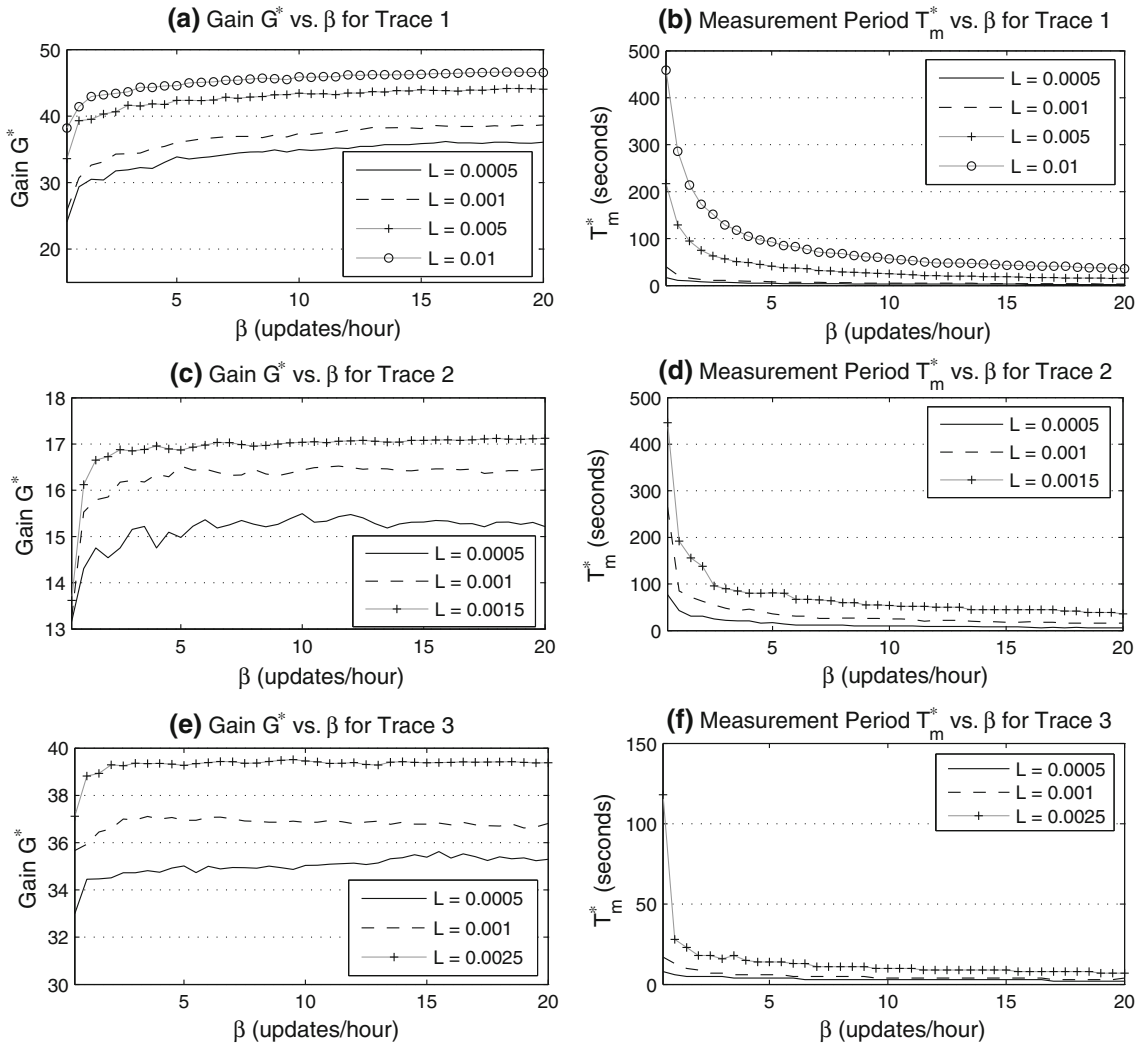

Fig. 5 Gain G^* and measurement period T_m^* values as a function of desired maximum update rate β for different values of loss rate L and for traces 1, 2, and 3

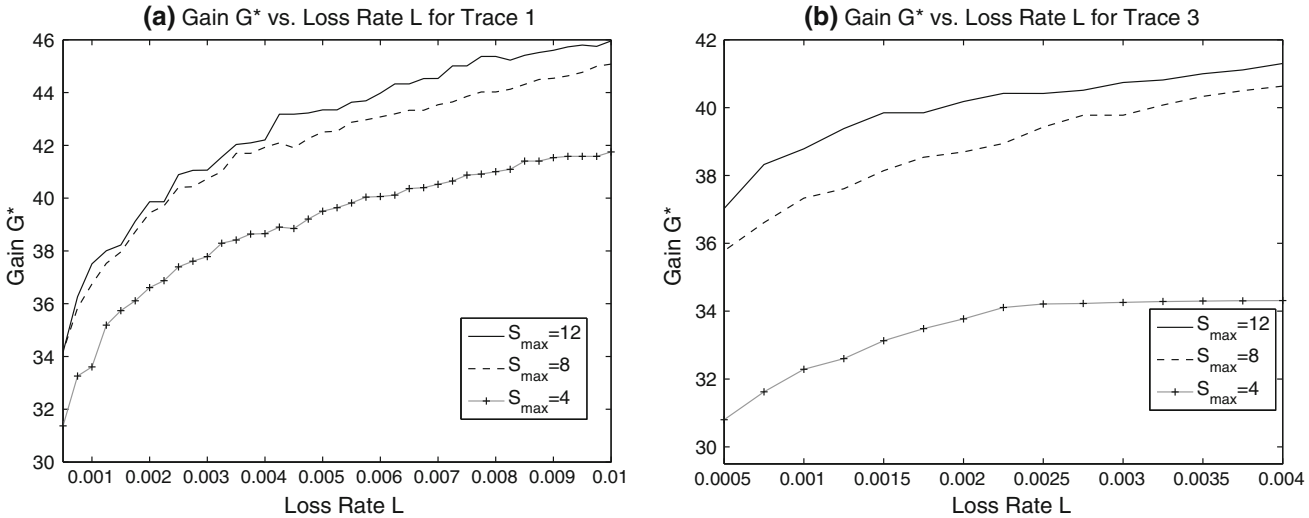

Fig. 6 The gain G^* as a function of the loss rate L for three different values of $S_{\max}$ and $\beta = 6$ for **a** Trace 1 **b** Trace 3

the benchmark OSWA algorithm uses the best measurement period T_m^* through the offline procedure. In all cases, LC-OSWA is able to approximately attain the desired loss rate L_T and the gain obtained by LC-OSWA is similar to that obtained by the offline procedure based on OSWA. Therefore, we conclude that the online algorithm LC-OSWA can safely be used to attain high bandwidth gains while maintaining a desired loss rate without a need for offline calculations.

Finally, we demonstrate the behavior of T_m as a function of h, index for the observation period, when LC-OSWA algorithm is used for two combinations of L_T and β values. For this purpose, trace 1 is concatenated with itself three times to obtain a 201-h-long data. In both scenarios, we observe that T_m hovers around in the vicinity of T_m^*, which is calculated offline; see Fig. 7. Therefore, we conclude that the LC-OSWA algorithm effectively finds the needed measurement period just using online loss rate measurements.

Table 2 LC-OSWA versus OSWA comparison for trace 1 for $L_T = 0.001$

β	LC-OSWA			OSWA	
	Loss rate L	Update rate	Gain G	G^*	Update rate
0.5	0.0014	0.51	27.00	27.45	0.51
1	0.0013	1.00	31.71	30.92	1.00
2	0.0011	2.01	34.83	33.36	2.03
4	0.0011	4.01	37.01	34.76	4.00
8	0.0010	8.00	38.92	36.35	8.00
16	0.0011	15.87	40.68	38.05	15.92

Table 3 LC-OSWA versus OSWA comparison for trace 1 for $L_T = 0.01$

β	LC-OSWA			OSWA	
	Loss rate L	Update rate	Gain G	G^*	Update rate
0.5	0.0096	0.50	40.30	38.83	0.50
1	0.0100	1.00	41.13	42.73	1.00
2	0.0096	1.95	43.82	43.06	1.89
4	0.0098	3.77	44.64	44.29	3.60
8	0.0091	7.27	45.50	45.57	6.73
16	0.0094	13.18	46.65	46.41	12.16

Table 4 LC-OSWA versus OSWA comparison for trace 3 for $L_T = 0.001$

β	LC-OSWA			OSWA	
	Loss rate L	Update rate	Gain G	G^*	Update rate
0.5	0.0011	0.50	35.92	35.92	0.50
1	0.0010	1.00	36.20	36.25	0.99
2	0.0010	1.94	36.55	36.53	1.91
4	0.0011	3.75	37.15	37.14	3.87
8	0.0009	7.55	36.95	37.58	7.20
16	0.0010	15.15	36.96	37.61	15.33

Table 5 LC-OSWA versus OSWA comparison for trace 3 for $L_T = 0.0025$

β	LC-OSWA			OSWA	
	Loss rate L	Update rate	Gain G	G^*	Update rate
0.5	0.0026	0.49	37.38	37.46	0.49
1	0.0028	0.89	38.58	39.15	0.90
2	0.0025	1.68	38.99	39.21	1.77
4	0.0023	3.07	39.14	39.26	3.00
8	0.0027	5.23	40.57	39.42	5.18
16	0.0028	10.03	40.61	39.50	9.83

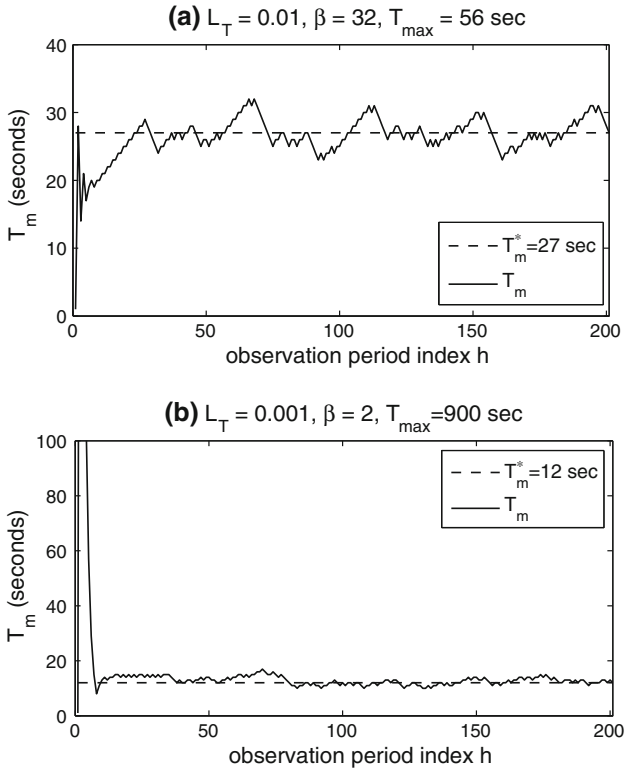

Fig. 7 Measurement period T_m depicted as a function of observation period index h for LC-OSWA for trace 1 in comparison with the measurement period T_m^* calculated offline for the cases **a** $L_T = 0.01$, $\beta = 32$ and **b** L_T=0.001, $\beta = 2$ with both scenarios using $T_{\max} = T_u/2$

4 Conclusions

An online slot width adjustment mechanism OSWA is proposed for flexgrid networks to map time-varying IP traffic to a flexi-path by varying the slot width with respect to the traffic variations in time. While doing so, a desired slot width

update rate is enforced in order to maintain the associated signaling load at acceptable levels. While OSWA presents significant bandwidth gains, it can not control the loss rate, which is inevitable. We also propose a loss-controlled version of OSWA, called LC-OSWA, that maintains a tolerable loss rate based on online loss measurements. Through three publicly available traffic traces, we show that LC-OSWA not only maintains a certain tolerable loss rate but also complies with the update rate constraint but still presenting significant bandwidth gains. Further studies are necessary that make use of actual or synthetic traffic traces with different characteristics (such as 1 Tbps traces) than the ones studied in this paper to explore the benefits and limitations of the proposed approach. Another important research direction for future work is to study if bandwidth gains obtained at the flexi-path level can also be harvested at the network level with effective routing and spectrum allocation mechanisms in place.

References

[1] Akar, N., Toksöz, M.A.: MPLS Automatic Bandwidth Allocation via Adaptive Hysteresis. Comput. Netw. **55**(5), 1181–1196 (2011)

[2] Anjali, T., Scoglio, C., Uhl, G.: A new scheme for traffic estimation and resource allocation for bandwidth brokers. Comput. Netw. **41**(6), 761–777 (2003)

[3] Battestilli, T., Perros, H.: An introduction to optical burst switching. IEEE Commun Mag **41**(8), S10–S15 (2003)

[4] CAIDA: The equinix-chicago Internet data collection monitor located at the Equinix datacenter in Chicago, IL (2011). http://www.caida.org/data/monitors/passive-equinix-chicago.xml

[5] Castro, A., Velasco, L., Ruiz, M., Klinkowski, M., Fernández-Palacios, J.P., Careglio, D.: Dynamic routing and spectrum (re) allocation in future flexgrid optical networks. Comput. Netw. **56**(12), 2869–2883 (2012)

[6] Cho, K., Mitsuya, K., Kato, A.: Traffic data repository at the WIDE project http://mawi.wide.ad.jp/mawi. In: Proceedings of the Annual Conference on USENIX Annual Technical Conference, pp. 51–51. USENIX Association Berkeley, CA, USA (2000)

[7] Cho, K., Mitsuya, K., Kato, A.: Traffic data repository at the WIDE project//mawi.wide.ad.jp / mawi / samplepoint-F/2009/200901011400. In: Proceedings of the Annual Conference on USENIX Annual Technical Conference, pp. 51–51. USENIX Association Berkeley, CA, USA (2000)

[8] Christodoulopoulos, K., Tomkos, I., Varvarigos, E.: Routing and spectrum allocation in OFDM-based optical networks with elastic bandwidth allocation. In: Global Telecommunications Conference (GLOBECOM 2010), 2010 IEEE (2010)

[9] Christodoulopoulos, K., Tomkos, I., Varvarigos, E.: Elastic bandwidth allocation in flexible OFDM-based optical networks. J Lightwave Technol **29**(9), 1354–1366 (2011)

[10] Dasgupta, S., de Oliveira, J.C., Vasseur, J.P.: Dynamic traffic engineering for mixed traffic on international networks: simulation and analysis on real network and traffic scenarios. Comput. Netw. **52**(11), 2237–2258 (2008)

[11] de Dios, O.G., Casellas, R., Zahang, F., Fu, X., amd I. Hussein, D.C.: Framework and Requirements for GMPLS based control of Flexi-grid DWDM. Internet Engineering Task Force . Internet-Draft draft-ietf-ccamp-flexi-grid-fwk-00.(2013)

[12] Geisler, D.J., Proietti, R., Yin, Y., Scott, R.P., Cai, X., Fontaine, N., Paraschis, L., Gerstel, O., Yoo, S.J.B.: The first testbed demonstration of a flexible bandwidth network with a real-time adaptive control plane. In: 37th European Conference and Exposition on Optical Communications, p. Th.13.K.2. Optical Society of America (2011)

[13] Geisler, D.J., Proietti, R., Yin, Y., Scott, R.P., Cai, X., Fontaine, N.K., Paraschis, L., Gerstel, O., Yoo, S.J.B.: Experimental demonstration of flexible bandwidth networking with real-time impairment awareness. Opt. Express. **19**(26), B736–B745 (2011)

[14] Gerstel, O.: Realistic approaches to scaling the IP network using optics. In: Optical Fiber Communication Conference and Exposition (OFC/NFOEC), 2011 and the National Fiber Optic Engineers Conference, pp. 1–3 (2011)

[15] Gerstel, O., Jinno, M., Lord, A., Yoo, S.J.B.: Elastic optical networking: a new dawn for the optical layer? IEEE Commun. Mag. **50**(2), s12–s20 (2012)

[16] ITU-T: Spectral grids for WDM applications: DWDM frequency grid. Recommendation G.694.1, International Telecommunication Union (2012)

[17] Jinno, M., Kozicki, B., Takara, H., Watanabe, A., Sone, Y., Tanaka, T., Hirano, A.: Distance-adaptive spectrum resource allocation in spectrum-sliced elastic optical path network. IEEE Commun. Mag. **48**(8), 138–145 (2010)

[18] Jinno, M., Takara, H., Kozicki, B., Tsukishima, Y., Sone, Y., Matsuoka, S.: Spectrum-efficient and scalable elastic optical path network: architecture, benefits, and enabling technologies. IEEE Commun. Mag. **47**(11), 66–73 (2009)

[19] Klinkowski, M., Ruiz, M., Velasco, L., Careglio, D., Lopez, V., Comellas, J.: Elastic spectrum allocation for time-varying traffic in flexgrid optical networks. IEEE J. Selec. Areas. Commun. **31**(1), 26–38 (2013)

[20] Krithikaivasan, B., Deka, K., Medhi, D.: Adaptive bandwidth provisioning envelope based on discrete temporal network measurements. In: IEEE INFOCOM, pp. 1786–1796. Hong Kong (2004)

[21] Levy, H., Mendelson, T., Goren, G.: Dynamic allocation of resources to virtual path agents. IEEE/ACM Trans. Netw. (TON) **12**(4), 746–758 (2004)

[22] Milbrandt, J., Menth, M., Kopf, S.: Adaptive bandwidth allocation for wide area networks. In: COST-279 Management Committee Meeting, Antalya, Turkey (2005)

[23] Mocci, U., Pannunzi, P., Scoglio, C.: Adaptive capacity management of virtual path network. In: IEEE Globecom, pp. 750–754. London (1996)

[24] Ohta, S., Sato, K.: Dynamic bandwidth control of the virtual path in an asynchronous transfer mode network. IEEE Trans. Commun. **40**(7), 1239–1247 (1992)

[25] Orda, A., Pacifici, G., Pendarakis, D.: An adaptive virtual path allocation policy for broadband networks. In: Proceedings IEEE INFOCOM'96. Fifteenth Annual Joint Conference of the IEEE Computer Societies. Networking the Next Generation, vol. 1 (1996)

[26] Pincemin, E.: Challenges of 40/100 Gbps deployments in long-haul transport networks on existing fibre and system infrastructure. In: Optical Fiber Communication (OFC), collocated National Fiber Optic Engineers Conference, 2010 Conference on (OFC/NFOEC), pp. 1–3 (2010)

[27] Rajagopalan, B., Luciani, J., Awduche, D.: IP over Optical Networks: A Framework. RFC 3717 (Informational) (2004). http://www.ietf.org/rfc/rfc3717.txt

[28] Rosa, A., Cavdar, C., Carvalho, S., Costa, J., Wosinska, L.: Spectrum allocation policy modeling for elastic optical networks. In: High Capacity Optical Networks and Enabling Technologies (HONET), 2012 9th International Conference on, pp. 242–246 (2012)

[29] Rouskas, G.N., Xu, L.: Optical packet switching. In: Sivalingam, K., Subramaniam, S. (eds.) Emerging Optical Network Technologies: Architectures, Protocols, and Performance, pp. 111–127. Springer, Norwell, Massachusetts (2004)
[30] Velasco, L., Klinkowski, M., Ruiz, M., Comellas, J.: Modeling the routing and spectrum allocation problem for flexgrid optical networks. Photonic Netw. Commun. **24**(3), 177–186 (2012)
[31] Wan, X., Wang, L., Hua, N., Zhang, H., Zheng, X.: Dynamic routing and spectrum assignment in flexible optical path networks. In: National Fiber Optic Engineers Conference. Optical Society of America (2011)
[32] Wang, R., Mukherjee, B.: Spectrum management in heterogeneous bandwidth optical networks. Optical Switching and Networking 11, Part A, 83–91 (2014)
[33] Wang, X., Zhang, Q., Kim, I., Palacharla, P., Sekiya, M.: Utilization entropy for assessing resource fragmentation in optical networks. In: Optical Fiber Communication Conference and Exposition (OFC/NFOEC), 2012 and the National Fiber Optic Engineers Conference (2012)
[34] Wang, Y., Zhang, J., Zhao, Y., Liu, J., Gu, W.: Spectrum consecutiveness based routing and spectrum allocation in flexible bandwidth networks. Chin. Optics Lett. S10,606 1–4 (2012)
[35] Yu, X., Zhang, J., Zhao, Y., Peng, T., Bai, Y., Wang, D., Lin, X.: Spectrum compactness based defragmentation in flexible bandwidth optical networks. In: Optical Fiber Communication Conference and Exposition (OFC/NFOEC), 2012 and the National Fiber Optic Engineers Conference (2012)
[36] Yumer, R., Akar, N., Karasan, E.: Class-based first-fit spectrum allocation with fragmentation avoidance for dynamic flexgrid optical networks. Opt. Switch. Netw. (2014). doi:10.1016/j.osn.2014.06.001
[37] Zhang, F., Zhang, X., Farrel, A., de Dios, O.G., Ceccarelli, D.: RSVP-TE Signaling Extensions in support of Flexible Grid. Internet Engineering Task Force (2013). Internet-Draft draft-zhang-ccamp-flexible-grid-rsvp-te-ext-03.txt.
[38] Zhang, G., De Leenheer, M., Morea, A., Mukherjee, B.: A survey on OFDM-based elastic core optical networking. IEEE Commun Surveys Tutorials **15**(1), 65–87 (2013)
[39] Zhang, J., Zhang, J., Zhao, Y., Yang, H., Yu, X., Wang, L., Fu, X.: Experimental demonstration of openflow-based control plane for elastic lightpath provisioning in flexi-grid optical networks. Opt. Express **21**(2), 1364–1373 (2013)

Caglar Tunc received the B.S. degree from Bilkent University in 2013 in electrical and electronics engineering. He is currently pursuing the M.S. degree in the same department. His current research interests are on the algorithmic aspects of computer and communication systems.

Nail Akar received the B.S. degree from Middle East Technical University, Turkey, in 1987 and M.S. and Ph.D. degrees from Bilkent University, Ankara, Turkey, in 1989 and 1994, respectively, all in electrical and electronics engineering. From 1994 to 1996, he was a visiting scholar and a visiting assistant professor in the Computer Science Telecommunications program at the University of Missouri - Kansas City. He joined the Technology Planning and Integration group at Long Distance Division, Sprint, Overland Park, Kansas, in 1996, where he held a senior member of technical staff position from 1999 to 2000. Since 2000, he has been with Bilkent University, Turkey, currently as an associate professor at the Electrical and Electronics Engineering Department. He visited the School of Computing, University of Missouri - Kansas City, as a Fulbright scholar in 2010 for a period of six months. His current research interests include performance analysis of computer and communication systems and networks, performance evaluation tools and methodologies, design and engineering of optical and wireless networks, queuing systems, and resource management.